

Doctoral (Ph.D.) Thesis

# **Kinetics of charge transfer at the charge transfer layer/halide perovskite interface**

**Xiangtian Chen**

Supervisors:

**Dr. Csaba Janáky**

Associate Professor

**Dr. Gergely Ferenc Samu**

Assistant Professor



**DOCTORAL SCHOOL OF CHEMISTRY**  
**University of Szeged**  
**Faculty of Science and Informatics**  
**Department of Physical Chemistry and Materials Science**

**Szeged**

**2025**

## 1. Introduction and aims

Lead halide perovskites (LHP) have received intensive attention in the past decades due to their easy synthesis, high absorption coefficient, long carrier diffusion length, and tunable bandgap. These materials are widely used as active materials in solar cells, light emitting diodes, photodetectors, and lasers. The extensive research effort boosted the power conversion efficiency of lead halide perovskite solar cells (PSCs) over 26% in a decade (**Figure 1**). With efficiencies approaching those of silicon single-junction solar cells, PSCs offer lower production costs due to the abundance of materials and low-temperature synthesis methods. The composition tunable light absorption of lead halide perovskites allows the preparation of tandem solar cells. These can utilize a wider range of the solar spectrum and achieve even higher conversion efficiencies than their single-junction counterparts (**Figure 1**). Additionally, lead halide perovskites can be deposited on a variety of substrates, including flexible ones, offering opportunities for wearable devices.

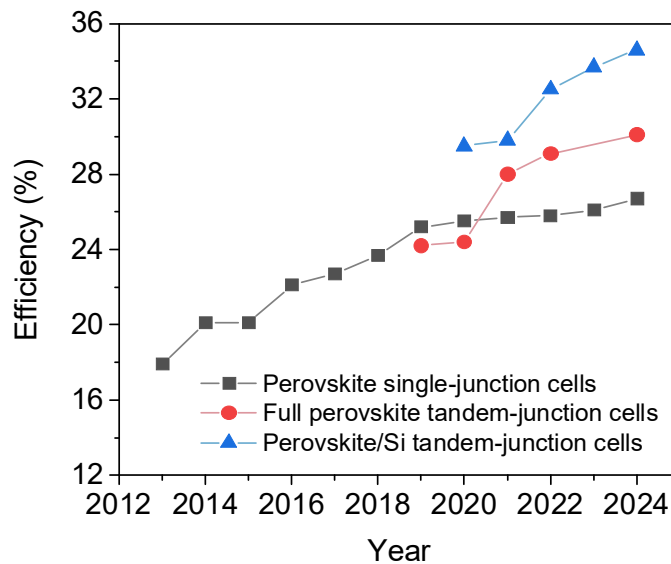


**Figure 1.** Improvement of perovskite solar cell efficiency (data extracted from NREL database).

PSCs typically have multiple components, namely a light absorption layer, electron extraction and hole layers, and metal contacts. In these architectures, the lead halide perovskite layer absorbs light and generates photo-excited charge carriers (electrons

and holes). Free electrons and holes can be transported to the charge transfer layer (CTL)/perovskite interface and in a subsequent step extracted and collected. Undesired carrier recombination at various trap states in the bulk and interfacial regions leads to carrier losses, deleteriously influencing carrier collection. To improve the efficiency (and stability) of PSCs, suppressing these carrier loss pathways is crucial. Current strategies focus on improving the quality (e.g., crystal quality and interface quality) of the lead halide perovskite layer and CTLs, passivating trap states both in the bulk and on the surface. The thermodynamic driving force behind efficient charge separation and extraction is related to the band energetics (band positions, alignment, and offset) at the CTL/LHP interface. However, as the charge extraction process is convoluted, exact design principles were not yet established. Some studies state that large band position offsets at CTL/perovskite interface are beneficial for assisting charge transfer. Other studies argue that smaller band position offsets at this interface facilitate smoother charge transfer.

By examining and understanding the fate of excited charge carriers design rules can be established that can aid the material choices for PSCs. Charge generation, recombination, and transfer processes typically occur on a short time scale (e.g., from fs to ns). Ultrafast techniques are required to track these processes, such as transient absorption spectroscopy (TA), time-resolved photoluminescence (TRPL), time-resolved microwave conductivity and transient surface photovoltage. Among them, TA and TRPL are the most commonly used techniques. Comparing the determined charge carrier transfer rate constants with these techniques, a large dispersion can be observed in the reported values, ranging from transit times between a few femtoseconds to tens of nanoseconds. Different factors can contribute to this variability, including sample properties, measurement parameters, measurement environment, and evaluation methodology. To further aid device design, it is crucial to understand the role these factors play in the determination of the charge carrier transfer rate constants and effort must be devoted to minimize the observed dispersion.

Built-in/applied electric fields present in PSCs can also influence charge carrier dynamics and device stability. Therefore, it is important to understand how the applied

electrical bias can influence charge separation, accumulation, and transfer. Operando spectroelectrochemical techniques can be used to monitor the influence of selective charge carrier injection in CTL/perovskite half-cell assemblies, with electron transfer layer (ETL) and hole transfer layer (HTL) separately. To reliably and accurately reveal the influence of external electric bias on the electron/hole injection process through the interfaces the electrochemical stability window of these perovskite layers must be determined (to avoid undesired phase/chemical changes of perovskite layer).

Throughout my research, I aimed to explore open scientific questions related to charge transfer at the CTL/perovskite interfaces:

- *How does the used analysis method influence the determined charge transfer rate?*
- *How can the dispersion of the determined charge transfer rate be rationalized?*
- *What is the influence of the band alignment at different single crystal TiO<sub>2</sub>/perovskite interfaces on the electron transfer rate?*
- *How does the band position of perovskite films influence the hole transfer rate at NiO/perovskite interfaces?*
- *How does applied electrical bias influence the hole transfer process at NiO/perovskite interfaces and will the band alignment conditions at the interface affect it?*

## 2. Experimental techniques

### Preparation of $\text{FA}_{0.83}\text{Cs}_{0.17}\text{Pb}(\text{I}_{0.83}\text{Br}_{0.17})_3$ thin films

The precursor solutions were mixed by adding chemicals in a stoichiometric ratio (0.1713 g FAI, 0.0530 g CsI, 0.4121 g  $\text{PbI}_2$ , and 0.1123 g  $\text{PbBr}_2$ ) in 1 mL DMF and DMSO mixture solution (volume ratio 7:3) to form 1.0 M solution. Before spin coating, the solution was placed on a hot plate (70 °C) with continuous stirring for more than 1 hour. Then it was filtered with a 0.2  $\mu\text{m}$  PTFE filter. To achieve a thin perovskite film (~100 nm thickness), the solution was diluted to a final 0.3 M solution with pure DMF.

### Preparation of $\text{FA}_{0.83}\text{Cs}_{0.17}\text{PbI}_3$ and $\text{FA}_{0.83}\text{Cs}_{0.17}\text{Pb}(\text{I}_{0.6}\text{Br}_{0.4})_3$ thin films

0.3 M concentration solution was directly prepared by mixing 0.0159 g CsI, 0.0514 g FAI, and 0.1660 g  $\text{PbI}_2$  for  $\text{FA}_{0.83}\text{Cs}_{0.17}\text{PbI}_3$  and 0.0159 g CsI, 0.0793 g  $\text{PbBr}_2$ , 0.0514 g FAI, and 0.0664 g  $\text{PbI}_2$  for  $\text{FA}_{0.83}\text{Cs}_{0.17}\text{Pb}(\text{I}_{0.6}\text{Br}_{0.4})_3$  in DMF and DMSO mixture solution (volume ratio 91:9). Identical heating, stirring and filtering procedure was carried out as  $\text{FA}_{0.83}\text{Cs}_{0.17}\text{Pb}(\text{I}_{0.83}\text{Br}_{0.17})_3$  before spin coating for both compositions.

### Spin coating of the perovskite thin films

Before spin coating, the substrates were subjected to UV ozone and oxygen plasma treatment for 20 min. For the first step, the perovskite precursor solution (50  $\mu\text{l}$ ) was uniformly spread on the substrate. The spin coating procedure contains two steps. In the first step, 1000 rpm spinning speed was used for 10 s (1000 rpm acceleration), and 4000 rpm spinning speed was used for 30 s (1200 rpm acceleration) in the second step. To assist crystallization, 100  $\mu\text{l}$  of chlorobenzene was dynamically dispensed on the substrate at the last 10 seconds of the spin coating procedure. Afterwards, the sample was placed on a hot plate for 2 min to form the perovskite phase. For the  $\text{FA}_{0.83}\text{Cs}_{0.17}\text{Pb}(\text{I}_{0.83}\text{Br}_{0.17})_3$  and  $\text{FA}_{0.83}\text{Cs}_{0.17}\text{Pb}(\text{I}_{0.6}\text{Br}_{0.4})_3$ , 80 °C of annealing temperature was used, while 120 °C was needed for  $\text{FA}_{0.83}\text{Cs}_{0.17}\text{PbI}_3$ , as the composition without Br incorporation requires higher temperature to achieve  $\alpha$ -phase. All preparation procedures were conducted in a glove box with a nitrogen atmosphere (<0.1 ppm  $\text{H}_2\text{O}$ ,

<10 ppm O<sub>2</sub>). The obtained perovskite layers were also stored under the same conditions.

### **Preparation of Mesoporous NiO hole transfer layer**

Mesoporous NiO HTLs were synthesized by galvanostatic electrodeposition. Before electrodeposition, the ITO substrates were cleaned by surfactant, and were then subjected to a three-steps of cleaning in deionized (DI) water, acetone and isopropanol (15 min for each sonication). The electrolyte was prepared by dissolving 0.13 M nickel sulfate, 0.13 M sodium acetate and 0.10 M sodium sulfate in DI water. The electrolyte was continuously stirred during the electrodeposition process. 0.5 mA cm<sup>-2</sup> of current density was applied. The layer thickness was controlled by varying the passed charges (30 mC cm<sup>-2</sup>, 60 mC cm<sup>-2</sup> and 120 mC cm<sup>-2</sup>). To obtain NiO, the as prepared films were annealed at 300 °C for one hour in air.

## **Characterization**

### **Steady state and time resolved photoluminescence (TRPL)**

Steady state and time resolved photoluminescence (TRPL) measurements were performed by Horiba DeltaPro with a 467 nm laser source. The applied laser pulse frequency during measurement was 500 kHz. This setup uses time-correlated single-photon counting (TCSPC) to record TRPL decaying curve.

### **Transient absorption spectroscopy (TA)**

Transient absorption spectroscopy measurements were performed using a pump-probe setup at the ELI ALPS Research Institute. The laser source was the HR-1 few-optical cycle laser system, with a repetition rate of 100 kHz. The system generates 1030 nm centered pulses (6-30 fs) having 1–2 mJ pulse energy. The laser consists of an ytterbium fiber chirped-pulse amplifier front end (250 W) and two postcompression stages, which compress the initial (270 fs) pulses to 30 fs and finally to 6 fs using the multipass cell technique. A fraction of the main beam was supplied to the TAS setup by using a beam splitter after the first postcompression stage. The laser pulse entering the setup was split

with a beam splitter in a 80/20 ratio, where 80% of the beam is used for pump beam generation and the remaining 20% generates the probe beam. The probe beam (white light) was generated by focusing the fundamental beam on a sapphire crystal. A Type I BBO crystal (Eksma Optics, 0.2 mm) was used to generate the pump beam (515 nm center wavelength).

### **UV-vis absorption spectroscopy**

Steady state UV-vis absorption spectra of the prepared perovskite layers on various substrates were measured by an Agilent 8453 UV-vis spectrophotometer. All measurements were carried out in a sealed cell under a nitrogen atmosphere.

### **Spectroelectrochemistry**

Spectroelectrochemistry is a powerful tool to track electrochemistry-induced processes that are accompanied by a color change. This color change can occur both in the electrolyte and on the surface of a transparent electrode. Simultaneously performing cyclic voltammetry (CV) and monitoring the sample absorption can be used to investigate the stability window of a perovskite electrode. A sealed three-electrode cell was used, with a perovskite layer as the working electrode, Pt wire as the counter electrode and a Ag/AgCl wire as a pseudo-reference electrode. The used electrolyte was 0.01 M Bu<sub>4</sub>NPF<sub>6</sub> DCM solution. CV was carried out by a Biologic VMP-300 potentiostat/galvanostat. Absorption measurement was carried out by an Agilent 8453 UV-visible spectrophotometer.

### **In-situ transient spectroelectrochemistry**

The same three-electrode system and electrolyte were used for the in situ transient spectroelectrochemistry measurements. Potentiostatic measurements, carried out by a Metrohm Autolab PGSTAT302 type potentiostat-galvanostat, was used to tune the Fermi level of NiO beneath the perovskite layer.

### **Contact potential difference (CPD)**

Contact potential difference (CPD) measurements were conducted by KP Technology

APS04. This technique was used to study the Fermi level and work function of a material. A vibrating gold tip, which has a constant Fermi level of  $-4.78$  eV, is used to form a capacitor with a grounded sample for contactless measurement of the potential difference between the two. The Fermi level of the sample can be determined by the following equation:

$$E_f(\text{sample}) = E_f(\text{gold tip}) + \text{CPD} \quad (1)$$

### **Surface photovoltage spectroscopy (SPS)**

Surface photovoltage spectroscopy (SPS) measurements were also conducted by KP Technology APS04. A monochromatic light illumination, with wavelength scanning from 1000 to 400 nm, was used during the measurement. Surface photovoltage can be determined by taking the difference between the recorded CPD values in the dark and under illumination.

### **Ambient-pressure photoemission spectroscopy (APS)**

Ambient-pressure photoemission spectroscopy (APS) was conducted by the same KP Technology APS04 instrument, but with a stationary gold tip. The grounded semiconductor sample was illuminated by a variable deep UV light source to liberate the electrons from the VB. The liberated electrons interact with the gas molecules in the atmosphere and form a cloud of negative ions. These negative ions have a much longer mean free path than the electrons. With an applied voltage, they can be collected by the sensor as a photocurrent. The onset photon energy of illuminated UV light can be determined as the VB position of the sample. However, VB signals are usually weak due to photoelectrons scattering with ambient gas. Cube root of photoemission is usually plotted to enhance the weak features.

### **Ultraviolet photoelectron spectroscopy (UPS)**

Ultraviolet photoelectron spectroscopy (UPS) was carried out by a He (I) photon source with an energy of 21.22 eV. Due to the low energy of applied photons, UPS is sensitive to the surface of the sample. This technique is conducted in ultra-high vacuum condition,



where a 10 V of electric bias was applied to collect secondary electrons. The kinetic energy of collected electrons will be recorded to determine the Fermi level and the VB position of the sample.

#### **Atomic force microscopy (AFM)**

Atomic force microscopy (AFM) images were recorded using a NT-MDT Solver AFM microscope to analyze the surface roughness of the single crystal TiO<sub>2</sub> substrates.

#### **Scanning electron microscopic (SEM)**

Scanning electron microscopic (SEM) images were measured by a FEI Helios NanoLab DualBeam instrument to record the morphology and grain size distribution of perovskite layers.

#### **X-ray diffraction (XRD)**

X-ray diffraction (XRD) patterns were measured with a Bruker D8 Advance instrument to analyze the phase purity of the samples. Cu K $\alpha$  ( $\lambda = 1.5418 \text{ \AA}$ ) was used for X-ray source. The measurement angle ranged from 10-80° for single crystal TiO<sub>2</sub> and 10-46° for perovskite layers. The scan speed was set to be 1° min<sup>-1</sup>.

## **Summary of new scientific results**

**T1: A large dispersion of the reported charge transfer rates (determined by time-resolved techniques) found in the literature for various charge transfer layer/perovskite interfaces (e.g. TiO<sub>2</sub>/perovskite).**

We summarized the reported charge transfer rates (with a dispersion from 0.8 ps to 100 ns) at charge transfer layer/perovskite interfaces determined by time-resolved techniques. Such dispersions occur in both electron transfer processes (e.g., at the TiO<sub>2</sub>/perovskite interface) and hole transfer processes (e.g., at the Spiro/perovskite interface), regardless of whether the charge transport layer has a planar or mesoporous structure. We identified such dispersion mainly came from three aspects: (i) sample properties, (ii) measurement parameters, and (iii) analysis methods.

**T2: Apart from sample properties and measurement conditions, the kinetic analysis used to interpret the relaxation of the excited state has a large contribution in the observed dispersion of charge transfer rates.**

Different methods which are used frequently in the literature, were evaluated on the same dataset for both TAS and TRPL measurements. After multiexponential fitting of the decay traces the charge transfer rate constant was extracted from (i) as one of the exponents from the multi-exponential fits, (ii) by solving the charge transfer equation or (iii) as the exponent of a stretched exponential fits. By using these methods different charge extraction rate constants were obtained (0.2- 14.1 ns), that we could link to be one of the causes behind the dispersion in the literature. To minimize the dispersion and to obtain comparable results, we suggest that a physical charge transfer model needs to be established first before attempting to analyze the kinetic traces. While model is unsure, the average lifetime, which is model independent, can be analyzed to showcase charge transfer.

**T3: The specific orientation of single crystal TiO<sub>2</sub> electron transfer layer influences the electron extraction rate from lead-halide perovskite layers.**

We have experimentally determined the energy level diagrams of the different orientations of the TiO<sub>2</sub> single crystals and perovskite by UPS and UV vis absorbance spectra. A larger CB offset ( $\Delta E = 1.0$ ) at the TiO<sub>2</sub> (100)/perovskite and TiO<sub>2</sub> (111)/perovskite interfaces can be observed compared to the offset at the TiO<sub>2</sub> (110)/perovskite interface ( $\Delta E = 0.4$ ). Time-resolved photoluminescence results reveal electron extraction kinetic is faster at the single crystal TiO<sub>2</sub>/perovskite interface with larger CB offset ((100) and (111)), and it is slower at the interface with smaller band offset (110).

**T4: There is an electrical barrier at the interface of TiO<sub>2</sub>/perovskite, which can be overcome by increasing the charge carrier density at the interface.**

The intermediate timescale of electron transfer was evaluated by TAS measurements. At low excitation fluences (0.7, 2.8  $\mu\text{J}/\text{cm}^2$ ), no sign of electron transfer was observed from the decay kinetics of all single crystal TiO<sub>2</sub>/perovskite samples when comparing to that of glass/perovskite sample. With low excitation fluence, the accumulated electrons at the conduction band have not enough energy to overcome the electrical barrier at TiO<sub>2</sub>/perovskite interface. In stark contrast when the excitation fluence is increased to 5.7  $\mu\text{J}/\text{cm}^2$ , the decay kinetics of single crystal TiO<sub>2</sub>/perovskite become faster than that of glass/perovskite, indicating enough electron accumulation is formed at this excitation fluence to overcome the electrical barrier and initiate electron transfer.

**T5: The overall kinetics of the electron extraction (ns timescale – free electrons) at the TiO<sub>2</sub>/perovskite interface strongly depends on the early extraction processes (ps timescale - hot-carriers).**

Hot carrier temperature determination in the early time scale of transient absorption spectroscopy data (ps range) reveals that hot carrier extraction is also faster at the interface with a larger conduction band offset. This can result in a relatively high concentration of electrons in the CB of TiO<sub>2</sub> (100) after 1 ps, which can bottleneck longer timescale electron extraction events, leading to slow electron extraction kinetic in the time range of 1-6 ns at this TiO<sub>2</sub> orientation (TAS results). In longer timescales

(TRPL results (in the time range of  $\sim 300$  ns)), when the electrons can be removed from the CB of  $\text{TiO}_2$  by either diffusing away from the interface or participating in back electron recombination events, efficient band edge electron extraction can be achieved by the  $\text{TiO}_2$  (100) facet again.

**T6: The electrochemical stability window was determined for two hybrid organic inorganic perovskites ( $\text{FA}_{0.83}\text{Cs}_{0.17}\text{PbI}_3$  and  $\text{FA}_{0.83}\text{Cs}_{0.17}\text{Pb}(\text{I}_{0.83}\text{Br}_{0.17})_3$ ) using spectroelectrochemical measurements.**

$\text{Bu}_4\text{NPF}_6/\text{dichloromethane}$  was used as an electrolyte to conduct spectroelectrochemical measurements. Results revealed multiple redox events coupled to distinct absorbance change of the layers outside the stability window. Ultimately, a stability window of  $-0.5\text{ V} - +0.5\text{ V}$  vs  $\text{Ag}/\text{AgCl}$  was determined for both  $\text{FA}_{0.83}\text{Cs}_{0.17}\text{PbI}_3$  and  $\text{FA}_{0.83}\text{Cs}_{0.17}\text{Pb}(\text{I}_{0.83}\text{Br}_{0.17})_3$ . Inside the stability window, the perovskite samples can stay stable for more than 4000 seconds.

**T7: The valence band position of perovskite layers influences the hole transfer rate to mesoporous  $\text{NiO}$  hole transfer layers.**

By incorporating different ratio of bromide content into  $\text{FA}_{0.83}\text{Cs}_{0.17}\text{Pb}(\text{I}_x\text{Br}_{1-x})_3$ , the valence band of perovskite can be lowered, creating larger VB offset at  $\text{NiO}/\text{perovskite}$  interface. The VB energy offset at different mesoporous  $\text{NiO}/\text{FA}_{0.83}\text{Cs}_{0.17}\text{Pb}(\text{I}_x\text{Br}_{1-x})_3$  interfaces were determined by ambient-pressure photoemission spectroscopy. Excitation fluence dependent TA measurements revealed that a larger VB offset can accelerate hole transfer process when segregation was under control.

**T8: Transient spectroelectrochemical measurements can be used to probe the influence of applied electrochemical bias on the rate of hole transfer at the  $\text{NiO}/\text{perovskite}$  interface.**

Transient spectroelectrochemical results revealed that applying a negative electrochemical bias can accelerate hole transfer process from perovskite layer to mp- $\text{NiO}$ , by depleting the holes in mp- $\text{NiO}$  layer (i.e. increase the Fermi level). In contrast,

applying a positive bias injects holes into mp-NiO (i.e. lowering the Fermi level), thus suppressing the hole transfer process at the interface. Furthermore, this effect of electrochemical bias was observed to be more pronounced at the NiO/perovskite interface with a larger VB offset.

## Scientific publications

Hungarian Scientific Bibliography (MTMT) identifier: 10076162

### Publications related to the scientific topic of the dissertation:

- 1) **Xiangtian Chen**, Krisztina Sárosi, Bálint Tóth, Barnabás Gilicze, Zsolt Bengery, Károly Mogyorósi, Csaba Janáky, Gergely Ferenc Samu, Electrochemical Modulation of Hole Extraction in NiO/Perovskite Bilayers. *Adv. Mater. Interfaces* **2025**, 10.1002/admi.202500159.

**IF2024 = 4.3**

- 2) **Xiangtian, Chen**, Prashant V. Kamat, Csaba Janáky, Gergely Ferenc Samu\*. Charge Transfer Kinetics in Halide Perovskites: On the Constraints of Time-Resolved Spectroscopy Measurements. *ACS Energy Lett.* **2024**, 9, 3187–3203.

**IF2024 = 19.3**

- 3) **Xiangtian, Chen**, Hannu P. Pasanen, Ramsha Khan, Nikolai V. Tkachenko, Csaba Janáky\*, Gergely Ferenc Samu\*. Effect of Single-Crystal TiO<sub>2</sub>/Perovskite Band Alignment on the Kinetics of Electron Extraction. *J. Phys. Chem. Lett.* **2024**, 15, 2057–2065.

**IF2024 = 4.8**

## Conferences

### Oral presentations:

- 1) **Chen Xiangtian**, Csaba Janáky, Gergely Ferenc Samu. The effect of single crystal TiO<sub>2</sub>/perovskite band alignment on the kinetics of electron extraction.  
XLVI. Chemistry Lectures, 17-19, October 2023, Szeged, Hungary.
- 2) **Chen Xiangtian**, Csaba Janáky, Gergely Ferenc Samu. Study of the effect of single crystal TiO<sub>2</sub>/perovskite band alignment on the kinetics of electron transfer.  
Solar2Chem conference, 18-22, September 2023, Tarragona, Spain.
- 3) **Chen Xiangtian**, Csaba Janáky, Gergely Ferenc Samu. Crystal facet dependent electron extraction at TiO<sub>2</sub>/perovskite revealed by time resolved spectroscopy  
Solar2Chem EPFL workshop, 22-24, May 2023, Lausanne, Switzerland
- 4) **Chen Xiangtian**, Csaba Janáky, Gergely Ferenc Samu. Investigation of electron extraction at TiO<sub>2</sub>/perovskite interface by time resolved spectroscopy.  
Solar2Chem Cambridge workshop, 6-9, December 2022, Cambridge, UK

### Poster presentations:

- 1) **Chen Xiangtian**, Csaba Janáky, Gergely Ferenc Samu. Crystal Facet Dependent Electron Extraction in TiO<sub>2</sub>/Perovskite Revealed by Time Resolved Photoluminescence and Transient Absorption Spectroscopy.  
Solar2chem Winter School, 22-24, February 2023, Valencia, Spain
- 2) **Chen Xiangtian**, Csaba Janáky, Gergely Ferenc Samu. The Application of Photoluminescence Spectroscopy in Perovskite Based Solar Cell/Photoelectrodes Study.  
Solar2Chem X Seafuel Symposium, 1<sup>st</sup>, April 2022, Tenerife, Spain